[AMERICAN JOURNAL OF SCIENCE, VOL. 282, OCTOBER, 1982, P. 1244-1263]

PYRITE TEXTURE, ISOTOPIC COMPOSITION AND THE AVAILABILITY OF IRON

R. RAISWELL

School of Environmental Sciences, University of East Anglia, Norwich, NR4 7TJ, England

ABSTRACT. Pyrite textures, isotopic compositions, and measurements of sediment reactive iron content have been studied on a radial traverse of pyritiferous carbonate concretions. An early framboidal pyrite formed throughout the sediment prior to concretionary growth from pore waters with a free diffusive connection to seawater and utilized in situ sources of reactive iron. Later euhedral pyrite was contemporaneous with concretionary growth and formed in a pore system with a restricted connection to seawater. Growth of euhedral pyrite occurred when in situ sources of iron were exhausted and required transportation of reactive iron from adjacent sediments. Changes in iron availability, pyrite texture, and crystallinity suggest an initially high level of supersaturation with respect to iron sulfides, with the preferred precipitation of iron monosulfide intermediates over pyrite leading to a framboidal texture. Subsequent euhedral pyrite formed by direct precipitation at lower degrees of supersaturation, such that pyrite was supersaturated, but iron monosulfides were undersaturated. The dependence of pyrite texture on iron availability is used together with isotopic data to define different pathways of pyrite paragenesis.

INTRODUCTION

Pyrite occurs in modern sediments and sedimentary rocks as single crystal euhedra (mainly cubes with some octahedra and pyritohedra) but also, and distinctively, as spheroidal aggregates of microcrystallites termed framboids (Love, 1964 and 1967). Studies of modern and ancient sediments initially emphasized the role of physical factors in producing the framboidal morphology, with suitable conditions believed to develop in spheroidal precursors comprised of micro-organisms, organic globules, iron sulfide gels or gaseous vacuoles (Love, 1957; Love and Amstutz, 1966; Rickard, 1970). However, laboratory syntheses have shown that the presence of spheroidal precursors is unnecessary (Berner, 1969a; Farrand, 1970; Sweeney and Kaplan, 1973), and origin of the framboidal texture apparently depends on chemical factors which influence the extent to which the metastable iron monosulfide intermediates (greigite, mackinawite) are involved in the formation of pyrite. In this paper an occurrence of framboidal and euhedral cubic pyrite is described where their clearly-defined temporal relationships permit the influence of chemical factors on texture to be partially evaluated.

It has been suggested that separate reaction pathways lead to framboidal or euhedral pyrite depending on the formation of metastable iron sulfide intermediates (Goldhaber and Kaplan, 1974). A summary of the proposed and observed reaction pathways is shown in figure 1. There appear to be two possible pathways for euhedral pyrite formation. Direct precipitation may occur when the pore water chemistry is such that pyrite

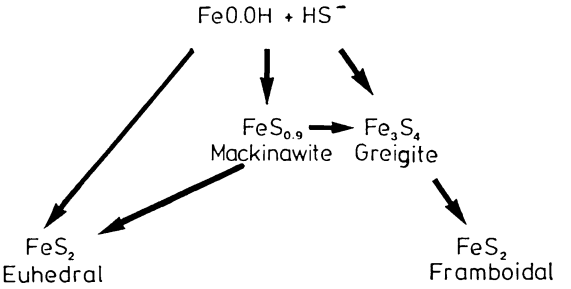

Fig. 1. Possible reaction pathways to framboidal and euhedral pyrite.

is supersaturated but precipitation of mackinawite or greigite is prevented by their undersaturation (Sweeney and Kaplan, 1973; Goldhaber and Kaplan, 1974). Alternatively euhedral pyrite may form by reaction between mackinawite and elemental sulfur (Goldhaber and Kaplan, 1974). This reaction has been observed to occur under anhydrous conditions at 150°C (Sweeney and Kaplan, 1973) and under aqueous conditions at 20° and 50°C in the presence of H_2S (Rickard, 1975). The kinetics of the latter reaction are consistent with pyrite precipitation by reaction between polysulfide ions (formed by the dissolution of elemental sulfur in sulfide solutions) and aqueous ferrous ions (produced by the dissolution of amorphous FeS).

Experimental syntheses of framboidal pyrite indicate that the texture develops inorganically during the reaction of iron monosulfides with elemental sulfur (Berner, 1969a; Farrand, 1970). The involvement of greigite appears to be crucial (Sweeney and Kaplan, 1973). Initial iron sulfide precipitates (sometimes identifiable as mackinawite) developed a spheroidal texture on transformation to greigite. During subsequent conversion to pyrite, the spheroidal texture could be retained or changed to a framboidal texture by internal nucleation of pyrite crystals. It has been suggested (Hallberg, 1972) that mackinawite is not necessarily a presursor to greigite and thus a framboidal texture may develop during the direct precipitation of greigite and its transformation to pyrite.

Sediment and pore water composition undoubtedly influence the extent and nature of the iron sulfide intermediates which may be formed and may thereby determine pyrite texture. The precise nature of this influence has not yet been ascertained, although Goldhaber and Kaplan (1974) have pointed out that the pH dependence of the products of reaction between sedimentary iron oxides and H_2S may reflect the relative solubility of mackinawite and pyrite. The solubility product of mackinawite has been measured by Berner (1967):

$$[Fe^{2+}]\,[S^{2-}] = Ksp_{mack} = 2.8 \times 10^{-18}\,.$$

Assuming saturation with orthorhombic sulfur, the solubility product of pyrite can be derived.

$$FeS_2 \rightleftharpoons Fe^{2+} + S^0 + S^{2-}$$

$$[Fe^{2+}]\,[S^{2-}] = Ksp_{pyrite} = 2.4 \times 10^{-28}$$

Since the activity of the sulfide ion is pH dependent, Goldhaber and Kaplan (1974) have suggested that, at high pH, solutions saturated with respect to both mackinawite and pyrite precipitate the former for kinetic reasons, despite the larger supersaturation of pyrite. However at low pH mackinawite may become undersaturated whereas pyrite, with its smaller solubility product, may still be supersaturated and may precipitate without competition. The influence of sediment and pore water composition may therefore control the formation of iron monosulfide intermediates and hence influence pyrite texture. In the present study, variations in sediment chemistry can be correlated with the changes in pyrite texture and isotopic composition defined across radial traverses of carbonate concretions.

SAMPLE DESCRIPTION

The locality.—Two pyritiferous carbonate concretions were collected from an outcrop of the Jet Rock (Upper Lias, Lower Jurassic) on the northeast coast of Yorkshire, England. At Port Mulgrave (NZ 799179), 11 km northwest of Whitby, the Jet Rock consists of fine-grained, well-laminated, organic-rich shales in which four main concretion-bearing horizons have been described and numbered by Howarth (1962). The sedimentological and paleoecological characteristics of these sediments have been discussed by Morris (1980).

A concretion was collected from each of two horizons: concretion UA came from bed number 33 (the Cannonball Doggers) and concretion UB from bed number 37 (the Curling Stones). The Cannonball Doggers range from flattened, elongate bodies to regular ellipsoids (30 cm max diam), whereas the Curling Stones are rather larger (70 cm max diam) and are commonly oblate spheroids. In each case the host sediment is differentially compacted around the concretion. These concretions have already been studied from a variety of aspects, including major element geochemistry (Raiswell, 1976), spatial distribution (Raiswell and White, 1978), trace element chemistry of the concretionary pyrite (Raiswell and Plant, 1980), and isotopic chemistry of the carbonate, organic matter, and sulfide phases (Coleman and Raiswell, 1981). These studies, in conjunction with the field evidence, indicate that the concretions grew during early diagenesis and were cemented in uncompacted sediment.

Sampling pattern.—Concretions were prepared for analysis as follows. Each concretion was cut open, and a slice removed from its center, parallel to the bedding plane (fig. 2). This slice was further sub-divided into a series of samples lying in concentric zones (identified by i, ii, et cetera). All the concentric zones, except the central one, contain four different samples. This sampling scheme and the samples themselves are those used by Raiswell (1976), who showed that the concretions exhibited radially symmetric compositional variations. Thus it was not necessary to analyze

all the samples, and a representative edge-center-edge traverse was chosen for each concretion. Appropriate host sediment samples of each bed were also analyzed.

Mineralogy and petrography.—X-ray powder diffraction was used to establish the mineralogy of samples from both the concretions and host sediments. In the concretions, the major authigenic minerals were calcite and pyrite (together constituting approx 80 to 90 percent by weight), accompanied by a detrital fraction consisting mainly of quartz and a 10Å (illitic) clay mineral. The host sediment mineralogy was similar except that calcite plus pyrite constituted only 10 to 30 percent, quartz 10 percent, with the remainder mostly illitic clays.

In thin section the Jet Rock sediments are finely-laminated organic-rich shales containing abundant pyrite framboids (<20 μm diam) in a matrix consisting of clays, amorphous organic matter, and silt-sized quartz grains. The carbonate cement in the concretion has a microsparite texture which completely envelopes shell material. Shell material is rather more abundant in the concretion than in the host sediments. The non-carbonate fractions of the concretions and host sediments resemble each other, except for the greater abundance of pyrite in the former.

Samples from the two concretions were examined by reflected light microscopy. The sulfide phase consists exclusively of pyrite, but two distinct textural varieties can be distinguished where it is disseminated. The textural differences are illustrated in plate 1-A,-B,-C for concretion UB. Plate 1-A shows the two main pyrite textures, a framboidal type and a euhedral granular variety. At the center of UB the framboids have euhedral overgrowths, but no euhedral pyrite is found inside the framboids, suggesting that the framboidal pyrite formed first. As the total amount of pyrite increases toward the concretion margin there is no change in the

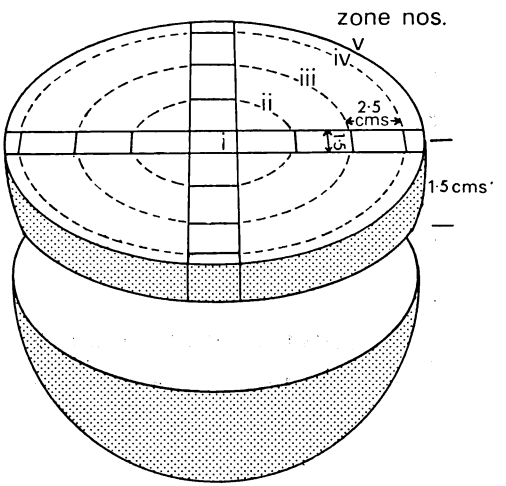

Fig. 2. The sampling pattern for concretions UA and UB.

PLATE I

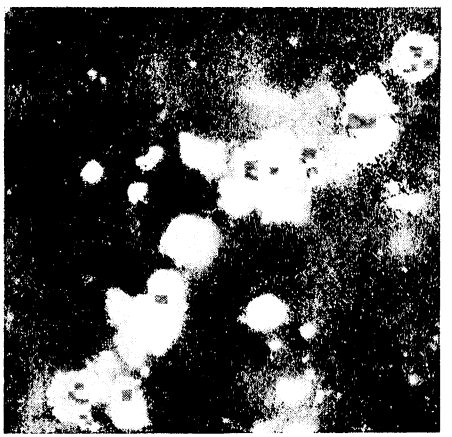

A. Central samples of concretion UB consist of framboidal pyrite with some euhedral overgrowths. Picture width 180 μm, oil immersion.

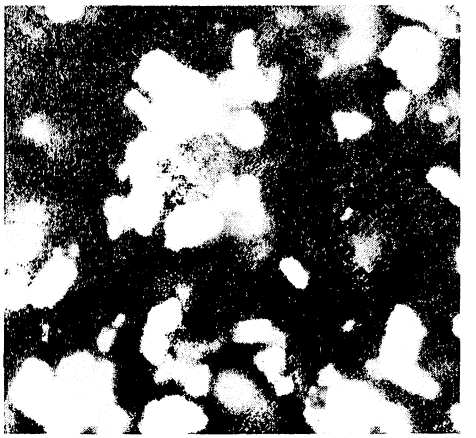

B. Framboidal pyrite becomes heavily encrusted with euhedra toward the concretion margin, and euhedral grains without obvious nuclei become increasingly abundant. Picture width 180 μm, oil immersion.

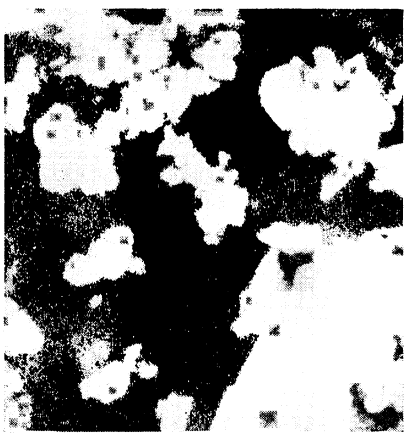

C. Grain boundaries disappear near the concretion margin and only rarely can framboidal remnants be detected in the euhedral aggregates. Picture width 180 μm, oil immersion.

abundance of framboids, although they become progressively overgrown with euhedral pyrite (pl. 1-B). Finally the euhedral crusts coalesce to form the pyrite margin of the concretion (pl. 1-C). The euhedra mostly appear to show sections of cubes, although octahedra have also been recognized.

The same spatial variations in texture are observed in concretion UA, but the central samples are more predominantly framboidal. Toward the concretion margin, euhedral pyrite progressively nucleates on the framboids and becomes more abundant, until the euhedral crusts coalesce into the pyritic rim. There is no apparent change in the abundance of framboids as the total pyrite content increases. In the pyritic rim, most grain boundaries are eliminated, and there is no trace of the earliest framboidal phase. In the host sediments coarse euhedral pyrite cubes are conspicuous at the hand-specimen level, but at the microscopic level framboids are volumetrically more important. Limited chemical and isotopic data suggest that the euhedral pyrite in the host sediments is similar in origin to the euhedra in the concretion margin, but the recrystallization of framboids may also have been contributory and further work is in progress on this question. These large euhedra were hand-picked from the sediments before analysis to avoid any possible bias in the chemical and isotopic data.

ANALYTICAL METHODS

Data for the carbonate and sulfide contents of each sample are taken from Raiswell (1976). Carbonate contents were determined by solution in dilute acetic acid followed by analysis for cations by atomic absorption (Ca, Mg, Sr, Mn) and colorimetry (Fe). Summing these analyses and their carbonate equivalents gave the total carbonate content of each sample.

Sulfide sulfur was measured gravimetrically following the procedure of Maxwell (1968, p. 483). Samples for sulfur isotope measurements were treated with cold 10 percent HCl to remove the carbonate fraction and then washed and dried. Carbon dioxide (from organic matter) and sulfur dioxide (from sulfides) were produced by oxidation at 1070°C (Robinson and Kusakabe, 1975) and separated by fractional sublimation before measurement in separate Micromass 602-C mass spectrometers (Coleman and Raiswell, 1981).

Acid-soluble iron was extracted by the technique described in Berner (1970). Carbonate-free samples were boiled for one minute with 12N HCl, and the dissolved iron measured as the dipyridyl complex (Riley, 1958).

RESULTS AND INTERPRETATION

The analytical results are reported in table 1. Carbonate and sulfide contents are expressed as calcium carbonate and pyrite respectively, in accordance with the observed mineralogy. Sulfur isotope data are given in the usual notation, where

$$\delta^{34}S = \left[\frac{(^{34}S/^{32}S)\ \text{sample}}{(^{34}S/^{32}S)\ \text{standard}} - 1 \right] \times 1000$$

The sulfur isotope standard is Cañon Diablo troilite.

Complete edge-center-edge traverses for the chemical and isotopic data are illustrated in figure 3, which demonstrates that both concretions show similar radially symmetric zonations.

Sulfur isotopes and pyrite texture.—The center-edge traverses in concretion UA show consistent trends to heavier $\delta^{34}S$ values, from −24.0 to −2.56 and −3.04 per mil. In concretion UB the center-edge traverses at first trend to lighter $\delta^{34}S$ values (−8.05 to −14.46 and −13.05 per mil) before showing a rather larger change to heavier values (−4.99 and −5.50 per mil) at the margin, as in concretion UA.

During sulfate reduction, variations in sulfur isotope abundance can arise as a result of both equilibrium and kinetic fractionations. The effects of the latter predominate in the relatively rapid, low temperature process of bacterial sulfate reduction, causing the resultant pyrite to be depleted in the heavier isotope. The instantaneous isotopic fractionation for laboratory studies of sulfate reduction is inversely proportional to the rate of reduction (Harrison and Thode, 1958; Kaplan and Rittenberg, 1964) and lies in the range 0 to 46 per mil, with most results showing fractionations of 0 to 25 per mil. However the instantaneous isotopic fractionations exhibited by natural sulfides commonly range up to 70 per mil, with many results in the region of 50 per mil. Such very light $\delta^{34}S$ values in natural

TABLE 1

Mineralogical, isotopic, and chemical variations in concretions UA and UB and their host sediments. DOP = degree of pyritization (see text)

Sample no.	Zone no.	Mineralogical Composition % Calcite	% Pyrite	% Fe_{HCl}	$\delta^{34}S$‰	DOP	
UA 1	v	26.3	56.1	n.d.	− 2.56	—	edge
2	iv	85.7	1.95	0.21	−10.06	0.81	↑
3	iii	85.9	1.02	0.23	−20.39	0.67	|
4	ii	87.6	0.90	0.22	−24.28	0.66	|
5	i	87.5	0.79	0.20	−24.01	0.65	center
6	ii	87.1	0.81	0.20	−16.84	0.66	|
7	iii	86.5	0.90	0.22	−17.88	0.66	|
8	iv	86.5	1.53	0.21	−11.27	0.80	↓
9	v	25.6	57.6	n.d.	− 3.04	—	edge
Host sediment		5.77 ±0.29	7.16 ±0.12	0.70 ±0.02	−25.76 ±0.43	0.83 ±0.02	
UB 1	vi	53.6	27.1	n.d.	− 4.99	—	edge
2	v	74.1	6.47	0.11	− 7.12	0.96	↑
3	iv	87.4	2.34	0.11	−13.42	0.91	|
4	iii	84.7	1.95	0.12	−14.46	0.89	|
5	ii	81.4	2.00	0.12	−13.32	0.89	|
6	i	84.2	3.70	0.13	− 8.05	0.93	center
7	ii	85.4	2.06	0.10	−11.25	0.91	|
8	iii	85.0	2.13	0.13	−13.05	0.88	|
9	iv	84.7	2.38	0.12	−12.20	0.90	|
10	v	81.2	5.41	0.11	− 8.93	0.96	↓
11	vi	53.5	23.8	n.d.	− 5.50	—	edge
Host sediment		20.6 ±3.2	7.96 ±0.18	0.55 ±0.02	−23.14 ±1.93	0.87 ±.02	

n.d. = not determined. Outer parts of the concretions are highly pyritic and contain oxides formed by weathering.

Each sediment analysis shows the mean and standard deviation of three samples.

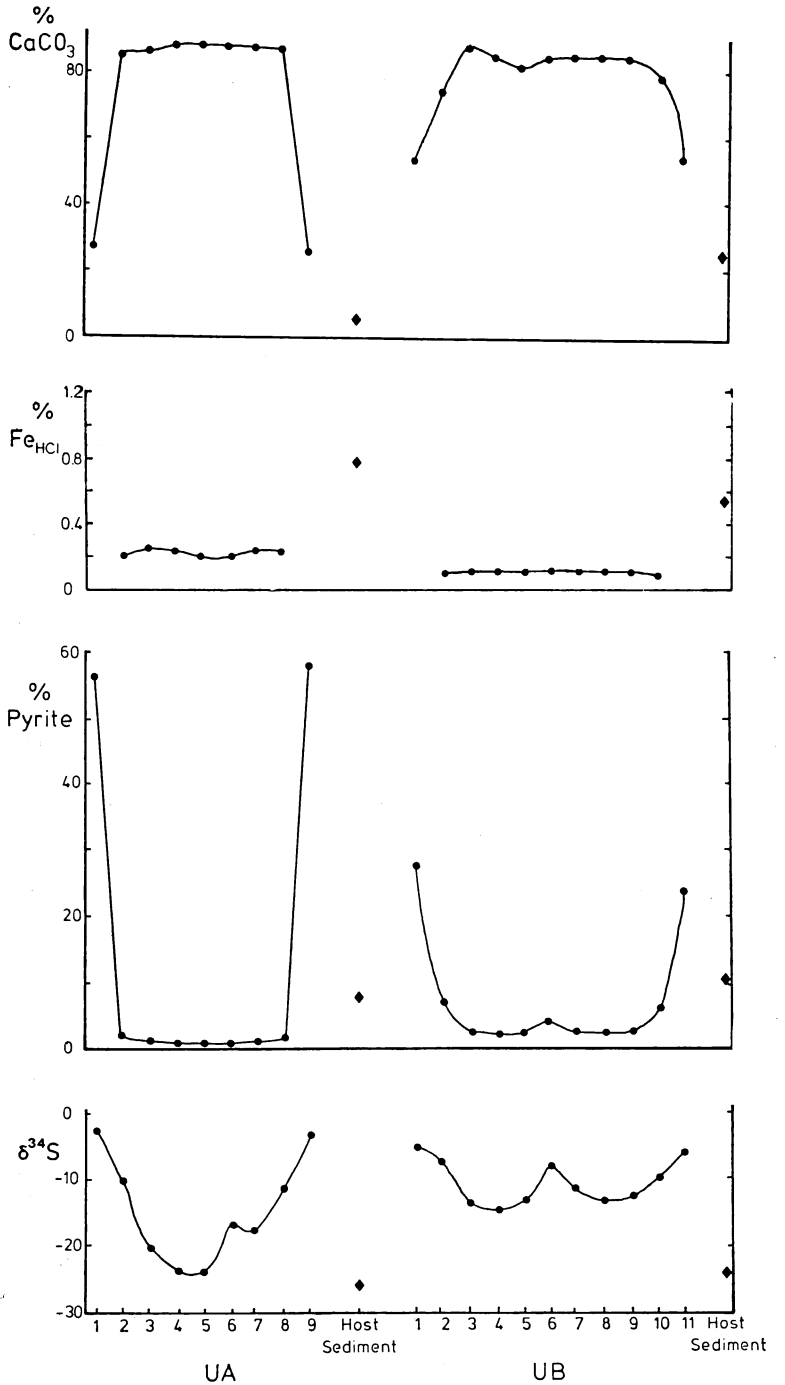

Fig. 3. Mineralogical, chemical, and isotopic variations on traverses of concretions UA and UB (●) and their mean host sediment composition (◆).

pyrites may result from the much slower rates of sulfate reduction in natural systems, as compared to laboratory systems (Rees, 1973; Trudinger and Chambers, 1973; Goldhaber and Kaplan, 1974).

The lightest values in concretion UA (−24 per mil) and the host sediments (−25.8 and −23.1 per mil) are consistent with a fractionation of −40 to −43 per mil with respect to Lias seawater sulfate at +17 per mil (Holser and Kaplan, 1966). This value lies within the fairly wide range (40-60 per mil) of instantaneous isotopic fractionations commonly observed between sulfate and sulfide in many near-surface sediments with access to an infinite source of seawater sulfate (Kaplan, Emery, and Rittenberg, 1963; Nakai and Jensen, 1964; Hartmann and Neilsen, 1969; Schwarz and Burnie, 1973; Goldhaber and Kaplan, 1974, 1975). However the extent of isotopic fractionation varies inversely with the rate of sulfate reduction, which in turn depends principally on organic matter reactivity (Berner, 1978). Organic matter reactivity decreases with increasing exposure to oxidation at the sediment-water interface (Berner, 1974; Goldhaber and Kaplan, 1975; Toth and Lerman, 1977), and hence rates of sulfate reduction are a function of sedimentation rates (Goldhaber and Kaplan, 1975; Berner, 1978). High sedimentation rates can therefore be correlated with lower isotopic fractionations (Goldhaber and Kaplan, 1975). The sedimentation rate of the Jet Rock has been estimated as 30 mm of compacted sediment per 1000 yr (Hallam, 1975), but scatter in the data of Goldhaber and Kaplan (1975) is too large to permit any useful estimate of the rate of sulfate reduction and hence the magnitude of the instantaneous isotopic fractionation from this sedimentation rate. Given the uncertainties in the data and the possibility that these Jet Rock samples may also have contained some later, isotopically heavy, pyrite the fractionation of −40 to −43 per mil indicates that these pyrites were mainly produced by sulfate reduction in an open system, with infinite access to sulfate in the overlying seawater.

The trend to heavier $\delta^{34}S$ values toward the concretion margin indicates that continued sulfate reduction occurred from a sulfate pool which became progressively heavier, as the lighter isotope was depleted. This change in the isotopic composition of the sulfate pool is due to changes in the relative rates of sulfate removal by reduction and sulfate supply by diffusion, which determine the degree of openness of the sediment with respect to transport from the overlying seawater. Thus sediments generally become more closed systems with depth, because the rate of sulfate reduction decreases with depth more slowly than does the diffusional flux of sulfate (Jorgensen, 1979). Completely open or closed systems are however endmember cases, and a strict interpretation of the isotopic data requires that the lightest values in concretion UB and host sediments (−24.2 to −25.8 per mil) occur in a prevailingly open system, where diffusion from seawater supplied a very large proportion of the sulfate for sulfate reduction. However isotopically heavier pyrites toward the concretion margin imply a more closed system, with a smaller proportion of the

reduced sulfate supplied by diffusion from the overlying seawater and more from within the sediment.

The isotopic data bear a close relationship to pyrite texture. The predominantly framboidal samples (host sediments and UA center) have the lightest $\delta^{34}S$ values (−24.2 to −25.8 per mil) and have clearly evolved in a prevailingly open system. Toward the margin of UA kinetic fractionation effects cause the $\delta^{34}S$ values of the total pyrite, and hence the euhedral pyrite, to become heavier as framboids of uniform abundance and isotopic composition are progressively overgrown by euhedra, in a sediment system that became more closed to seawater sulfate with depth.

The abundance of pyrite at the center of UA is similar to that in the host sediment, if account is taken for compaction of the sediment but not of the concretion. This can be done by comparing the proportions of pyrite present in the non-carbonate fractions of the concretion and host sediment, in effect crudely correcting for the dilution effect of the authigenic carbonate cement which preserved the concretion against compaction (Lippman, 1955; Raiswell, 1971). Pyrite contents expressed as a percentage of the non-carbonate fraction are quite similar in UA center (6.3 percent) and host sediments (7.6 ± 0.1 percent in three samples), considering that the isotopic data indicate that the host sediments may also contain some later pyrite. A similar conclusion on the relative abundances of pyrite in concretion and host sediment has been reached by Coleman and Raiswell (1981) by considering the relationships between $\delta^{34}S$ and total pyrite contents in concretions and host sediments.

The similarity of the pyrite phases at the center of UA and in its host sediment, in terms of both abundance and isotopic composition, provide cogent evidence for the occurrence of a dispersed phase of framboidal pyrite forming uniformly throughout the sediment prior to concretionary growth. The sediment pore system was sufficiently open to diffusive exchange with the overlying seawater to allow a significant degree of access for sulfate (and hence extensive pyritization) and egress for the alkalinity generated by sulfate reduction (Presley and Kaplan, 1968; Berner, Scott, and Thomlinson, 1970). The relatively open system with respect to alkalinity was probably responsible for the lack of carbonate precipitation and concretionary growth (Coleman and Raiswell, in preparation) at this stage. The nature of the pore system with respect to sulfide is determined mainly by the fraction of dissolved sulfide precipitated (Jorgensen, 1979) but must have been relatively closed as the most reactive iron phases would initially be available to stabilize sulfide within the sediment. However the subsequent phase of sulfate reduction occurred in a pore system that was more closed with respect to sulfate and alkalinity (as evidenced by the $\delta^{34}S$ values and the precipitation of carbonate cement in concretions) and resulted in a euhedral pyrite, which nucleated on framboids and became isotopically heavier toward the concretion margin.

The same temporal and isotopic relationships are present in UB but are partly obscured by variations in the abundance of the two types of pyrite. Host sediment pyrite (mainly framboidal) again has open system

$\delta^{34}S$ values, but the framboidal pyrite at the center of UB has euhedral overgrowths. Thus the total pyrite has a relatively heavy $\delta^{34}S$ value (−8.1 per mil). Away from the center there is an initial decrease in total pyrite content (and thus in the proportion of euhedra) which is reflected in the trend to lighter $\delta^{34}S$ values. Thereafter a progressive increase in total pyrite indicates an increasing proportion of euhedra and a trend to heavier $\delta^{34}S$ values. The pyrite contents expressed as a proportion of the non-carbonate fractions of the concretion center (23.4 percent) and host sediment (10.0 percent) are consistent with the interpretation that the former contains a greater proportion of the syn-concretionary euhedral pyrite, as compared to the pre-concretionary, mainly framboidal material.

Availability of iron.—Values of non-carbonate HCl-soluble iron are reported in table 1; there is little variation within either of the two concretions. Unfortunately values for acid-soluble iron in the outermost sample of each concretion could not be obtained, because subaerial weathering of the pyritic margin had produced iron oxides. However, there was no evidence of weathering in the remaining samples.

Berner (1970) considers that iron solubilized by this technique is present as fine-grained hematite, limonitic goethite, and chlorite with some contributions from coarser-grained iron oxides and silicates. The relative reactivity of these minerals toward H_2S was similar to their relative solubility in HCl, although greater quantities of iron may be solubilized by the latter unless the H_2S concentration is high. Iron soluble in HCl only therefore provides a comparative guide to the maximum amount of iron available for pyrite.

Values for non-carbonate HCl-soluble iron inside the concretions remain uniform, although the pyrite content of successive samples increases. This iron is therefore unreactive toward dissolved sulfide (at the concentrations that existed in the sediment), and increasing pyrite contents, due to the formation of euhedral pyrite, result from the addition of iron from an external source, rather than by the conversion of available iron to pyrite within the sediment sample.

A degree of pyritization (DOP) can be calculated (Berner, 1970)

$$\text{DOP} = \frac{\text{Wt \% Pyrite Fe}}{\text{Wt \% Pyrite Fe} + \text{Wt \% Acid-soluble Fe}}$$

Mainly-framboidal samples (UA center and inner) have the lowest DOP values (approx 0.65) which are rather higher than in modern pyrite sediments (DOP $\leqslant$ 0.44: Berner, 1970) where in situ sources of iron are inferred. However the sedimentological and paleoecological evidence (Morris, 1980) indicate that rates of sedimentation were relatively slow, compared to other Jurassic black shales, and that the oxic/anoxic boundary occurred at the sediment surface during deposition of the Jet Rock. These conditions would favor the high H_2S concentrations and extensive pyrite formation necessary to utilize a large proportion of available iron within the sediment. It is suggested accordingly that framboidal pyrite formed mainly from iron available within the sediment samples and that

changes in pyrite texture corresponded to changes in iron mobility. Initially iron from in situ sources was redistributed on a microscopic scale within the sediment to give framboidal pyrite, but subsequent euhedral pyrite formed from iron transported to the concretions over distances of many centimeters in the enclosing sediments.

Chemical models for pyrite formation.—Berner (1969b) has developed and tested experimentally a series of diagenetic models to explain the migration of iron and sulfur during early diagenesis. The most important controls are depth variations in organic matter content and the concentration of iron reactive toward H_2S. The models assume deposition of a thin organic-rich layer on a thicker section of organic-poor sediment. Subsequent behavior then depends on the molar ratio (R) of reactive iron to reducible sulfur (mainly pore water sulfate) at deposition. Values of $R < 0.4$, 0.4 to 10, and > 10 define respectively low, intermediate, and high iron content models. Assuming a depositional porosity of 85 percent for the Jet Rock (Raiswell, 1976), a liter of sediment plus porewater initially contained 0.024 mol $SO4^{2-}$ and 0.24 to 0.27 mol reactive iron (now host sediment pyrite). Thus $R \geqslant 10$, and the high reactive iron model is the appropriate analogue for the Jet Rock.

The chemical conditions that give rise to the variations in iron mobility recognized by Berner (1969b) in the high iron content model are illustrated in figure 4, with reference to the textural forms of pyrite found in the Jet Rock. The production of sulfide by bacterial sulfate reduction is initially very rapid, since reactive organic matter concentrations are a maximum, and the pore system is open to sulfate diffusion from overlying seawater (as indicated by the isotopic composition of the pre-concretionary pyrite). No significant degree of iron or sulfide migration is possible at this stage, because concentrations of both, buffered by equilibrium between reactive iron minerals and iron sulfide, are very low. Thus the rapid production of sulfide induces rapid precipitation of iron sulfide, using local or in situ sources of iron, and ultimately gives a dispersed phase of framboidal pyrite. Meanwhile, mobile reduced products of bacterial decay (for example, amines, aminoacids), which do not react rapidly, solubilize iron from adjacent sediment which is low in organic matter and hence create a concentration gradient transporting iron back to the organic-rich sediment layer. The addition of iron to the organic-rich layer from an adjacent layer results in the development of euhedral pyrite.

The correspondence of the high iron content model with the observed migration of iron in the Jet Rock has important implications for concretionary growth mechanisms, as well as for pyrite texture. The two-dimensional models of Berner (1969b) demonstrate that iron migration occurs where the sediments contain a heterogeneous distribution of organic matter, such that layers with a high organic content exhibit enhanced microbiological activity. In the three-dimensional case of the Jet Rock concretions, locally prolific sulfate reduction was responsible for the iron mobilization associated with euhedral pyrite and also for concretionary growth (Raiswell, 1976; Coleman and Raiswell, 1981). Clearly

the driving force for concretionary growth resulted from a concentration of organic matter at the site of the growing concretion, as already suggested by the associations of concretionary growth and fossil material (Weeks, 1953, 1957; Zangerl and others, 1969) and by experimental studies of microbiological carbonate precipitation (Berner, 1968). Suitable concentrations of organic matter might occur by the incorporation of organic carcasses within the Jet Rock, and the partial preservation of such material to act as sites for concretionary growth would be assisted by the absence of burrowing organisms and deposit feeders (Morris, 1979). The random distribution of carbonate concretions in the Jet Rock is consistent with this explanation (Raiswell and White, 1978) but the absence of skeletal

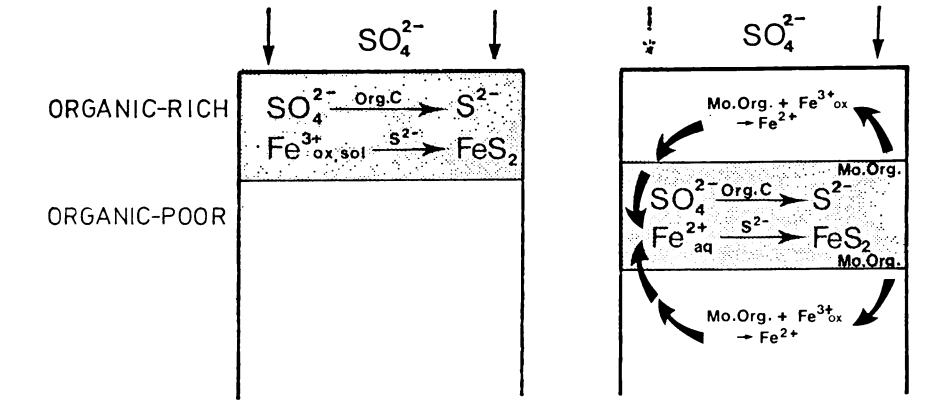

Time increasing →		
Reactants		
Org.C Reactivity	High	Low
Fe^{3+}_{ox} conc.	High	Absent
SO_4^{2-} conc.	High (open system)	Low (partially closed system)
Rate of Sulphate Reduction	Fast	Slow
Iron Mobility	Low	High
	Iron within system converted from oxide to sulphide	Iron added to system
Pyrite	FRAMBOIDAL	EUHEDRAL

Fig. 4. Relationship between pyrite texture and sediment chemistry. Organic matter reactivity is initially high, and the rapid production and precipitation of sulfide occurs, using the high concentrations of in situ, reactive iron and ultimately giving framboidal pyrite. Other reduced and dissolved products of bacterial decay (mobile organics or Mo. Org.) diffuse into adjacent sediments from which iron is solubilized for continued sulfide precipitation and the formation of euhedral pyrite.

remains within many concretions implies that soft-bodied organisms were mainly involved.

DISCUSSION

The models presented above suggest that the following factors may have influenced the development of pyrite texture in the Jet Rock:

1. the form of iron, whether an aqueous ferrous species or solid ferric phase, which reacts with dissolved sulfide;
2. reaction kinetics as determined by:
   A. rate of sulfate reduction, that is, sulfide generation,

and/or

   B. availability of iron.

The relative influences of these factors cannot be distinguished in the case of the Jet Rock pyrites, unless the data are considered in conjunction with observations from other pyrite-forming environments.

Considering (1), it is tempting to suggest that utilization of a within-sediment source of iron in framboid development implies the in situ sulfidation of iron oxides, initially to intermediate iron sulfide(s) through pathways on the right side of figure 1. However framboids may occur inside microfossils (Love, 1967), where the pores are smaller in diameter than the framboids and where in situ sources of iron would be absent or insufficient, and also as coarse aggregates (Emery, 1960; Sweeney and Kaplan, 1973). Such modes of occurrence strongly indicate that the dissolution and migration of iron occurred, as also implied by kinetic studies of goethite sulfidation to mackinawite (Rickard, 1974). Thus the formation of framboidal pyrite does not proceed by the in situ sulfidation of iron oxides.

There is, however, presumptive evidence that reaction kinetics are important in the larger grain-size and better crystallinity of the euhedral pyrite compared to the framboids, although it is impossible to distinguish the separate influences of rate of sulfate reduction and availability of iron, both of which are likely to have declined in the progression from framboidal to euhedral pyrite. Rates of sulfate reduction are strongly dependent on the abundance and quality of organic matter (Sweeney and Kaplan, 1973; Goldhaber and Kaplan, 1975; Toth and Lerman, 1977; Berner, 1978) and are almost certain to have declined in passing from the initial framboidal to later euhedral pyrite, simply because of progressive changes in the quality of the organic matter. Freshly-deposited organic matter has a high content of readily-metabolizable materials, which become exhausted with burial, and residual, more refractory material is associated with lower rates of sulfate reduction (Jorgensen, 1979; Berner, 1978). Thus the initial phase of framboidal pyrite apparently formed by decomposition of the most readily metabolized organic matter, dispersed throughout the sediment. Subsequent euhedral pyrite formed by the slower decomposition of local concentrations of organic matter, the lower quality of which allowed survival and burial. In contrast to the influence of organic matter, rates of sulfate reduction only become dependent on

sulfate concentration at relatively low levels (<10 mmol; Harrison and Thode, 1958; Kaplan and Rittenberg, 1964). However, the isotopic data show that the change in pyrite texture occurred at much higher sulfate concentrations, corresponding to the start of pore water depletion from seawater sulfate concentrations of 28 mmol (framboidal pyrite $\delta^{34}S$ −24 per mil, euhedral pyrite $\delta^{34}S$ >24 per mil). Thus any kinetic influence of sulfate reduction rate on pyrite texture was almost certainly due to changes in organic matter abundance and reactivity rather than sulfate concentration.

Changes in the availability of iron and their relationship to pyrite texture were discussed in the previous section, by analogy with the models of Berner (1969b). It is considered that these changes in iron availability might also affect the degree of saturation with respect to mackinawite ($Ksp = 2.8 \times 10^{-18}$; Berner, 1967) and pyrite ($Ksp = 2.4 \times 10^{-28}$; Goldhaber and Kaplan, 1974) and hence kinetically influence pyrite texture. In the presence of in situ sources of reactive iron, either as aqueous Fe^{2+} (activity $>10^{-5}$m) or as limonite, the dissolved H_2S activity in equilibrium with mackinawite is low ($<10^{-7}$m; Berner, 1969b). Hence rapid production of H_2S readily achieves saturation with respect to both pyrite and mackinawite. Despite the greater supersaturation of pyrite, Goldhaber and Kaplan (1974) have suggested that mackinawite may preferentially precipitate. During this phase of sulfide formation, comparatively high Fe^{2+} activities and FeS precipitation are effective in maintaining a low activity of dissolved H_2S, thus preventing loss by diffusion to adjacent horizons.

The first phase of sulfide formation occurred throughout the sediments in the concretionary horizon, causing a reduction in the degree of saturation of sulfides and depletion of in situ sources of reactive iron, with the following consequences for the subsequent phase of localized sulfide formation at concretionary sites. Firstly, mackinawite became undersaturated, whilst pyrite remained supersaturated. Direct precipitation of pyrite would then be possible, with the lower degrees of supersaturation giving coarse well-crystallized, euhedral products. Secondly, the ratio of Fe^{2+}:reduced sulfur decreased (as diffusion supply of Fe^{2+} replaced in situ sources), and H_2S became available to transform mackinawite to greigite and ultimately framboidal pyrite. Elemental sulfur or polysulfides are believed to be involved in this transformation (Berner, 1970; Rickard, 1975), and their formation is encouraged by the fluctuating redox conditions resulting from bioturbation. In the absence of bioturbation in the Jet Rock, elemental sulfur or polysulfides might form by reaction of goethite and H_2S (Goldhaber and Kaplan, 1974). Rates of Fe^{2+} supply by diffusion need not have matched rates of sulfide formation, and excess reduced sulfur could be lost as H_2S to the surrounding, lower pH sediments without inducing FeS precipitation.

The models offered here suggest that pyrites of different texture and isotopic composition can be arranged in a paragenetic sequence (fig. 5) in sediments where organic matter is heterogeneously distributed. Different

pathways are defined in the first instance by the extent of reactive iron availability relative to reduced sulfur. If sufficient in situ reactive iron is available for pore water supersaturation with respect to both pyrite and mackinawite, the preferential formation of the latter will ultimately lead to framboidal pyrite. This first pyrite phase will exhibit the maximum isotopic difference between pyrite and seawater sulfate in that system (dependent on the rate of sulfate reduction but typically 40-60 per mil). Provided sufficient reactive iron remains to maintain supersaturation with respect to mackinawite, the next pyrite phase will also be framboidal but will have heavier $\delta S^{34}S$ values as continued deposition gives a more closed system and depletion of the lighter isotope occurs. The same sequence of isotopic relations is found on the right side of figure 5, where the progression from isotopically light euhedra ($\Delta_{SO_4^{2-}}$ = 40-60 per mil) to heavier euhedra occurs. This sequence represents low concentrations of reactive iron either occurring in situ or being solubilized from adjacent horizons, as the pore system becomes prevailingly closed to sulfate diffusion. However the most interesting features of figure 5 are the cross-linkages between different textural types. As reactive iron becomes reduced or exhausted, pathways on the right side of figure 5 are favored, and framboids may be succeeded by euhedra either in systems prevailingly open or closed with respect to sulfate. Thus certain depositional and sedimentary environments may allow a maximum of three distinct phases of pyrite to develop under steady state conditions.

Not all reaction pathways or products are equally probable. Thus, most organic-rich sediments contain high concentrations of reactive iron

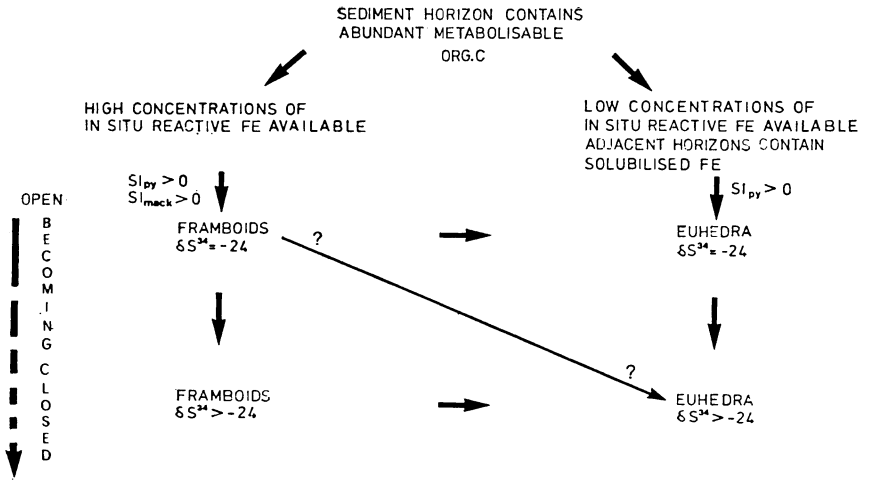

Fig. 5. Paragenetic relationships between pyrites of different texture and isotopic composition. Sulfate reduction in the presence of high concentrations of reactive iron gives oversaturation with respect to mackinawite and pyrite (SI_{mack}, $SI_{py} > 0$) and ultimately framboidal pyrite. Where iron can be solubilized from adjacent horizons (either by in situ formation of a reducing agent or diffusion of a reducing agent from the organic-rich horizon), lower degrees of sulfide saturation result in the formation of euhedral pyrite.

and will follow pathways starting from framboidal pyrite with prevailingly open system isotopic values. Subsequent development of isotopically heavy framboids is then more likely than open system euhedra, simply because the reduced organic products of sulfate reduction capable of solubilizing reactive iron are likely to escape in an open system rather than diffuse downward to adjacent horizons, where reactive iron is still available. Extensive development of open system euhedra would appear to be most probable where other microbiological processes, for example, fermentation, could solubilize iron from adjacent horizons where only limited sulfate reduction occurred. The transition from prevailingly open system framboids to prevailingly closed system euhedra occurs where the sediment becomes buried below the depth for diffusion to maintain isotopic homogeneity with seawater, whilst reactive iron concentrations are simultaneously reduced below the levels required for saturation with mackinawite (but are still such that pyrite is oversaturated). It seems probable that this diagonal pathway may really represent a collapsed sequence of open system framboids → open system euhedra → closed system euhedra or open system framboids → closed system framboids → closed system euhedra, where intermediate phases are poorly developed.

The relative proportions of the different textural and isotopic phases are controlled by those factors that affect:

A. the rate and magnitude of sulfide production, for example, availability of sulfate, rate of deposition, organic matter abundance, and reactivity;

B. the extent of iron sulfide saturation, for example, pore water sulfide concentrations, availability of in situ reactive iron, availability of reactive iron in adjacent horizons.

These factors may be to a large degree interrelated. The rate of sulfate reduction has been found to correlate with sedimentation rate in a variety of different depositional environments (Goldhaber and Kaplan, 1975), principally because sedimentation rate influences the reactivity of metabolizable organic matter and hence the rate of sulfate reduction. By contrast, concentrations of metabolizable organic matter apparently show rather little variation between different sediments (Berner, 1978) and may exert a correspondingly small influence on the rate of sulfate reduction. Sedimentation rate may be a useful master variable against which to examine changes in pyrite texture, because it may also exert a similar influence on iron reactivity as already found for organic matter. The presence of relatively reactive iron phases has the effect of stabilizing large proportions of H_2S as iron sulfides, thus reducing the diffusion loss rate (Jorgensen, 1979), and would be anticipated to correspond to excessive saturation levels with respect to iron sulfides and the development of framboidal pyrite. Conversely, less reactive iron phases would favor production of a euhedral phase. However the interplay of these factors is complex and cannot yet be assessed accurately. Thus the relationships in figure 5 are offered primarily as a framework for further investigations, although there are obvious difficulties in attempting to decipher details of

pyrite paragenesis. For example, in estuarine sediments undergoing non-steady state diagenesis, a range of products with complex temporal relationships would be anticipated.

SUMMARY AND CONCLUSIONS

1. Pyritiferous carbonate concretions from the Jet Rock (Upper Lias) contain two main types of pyrite: framboidal and euhedral. The abundances of each type, their petrographic relationships, and isotopic compositions indicate that growth of framboidal pyrite preceded the euhedral form. The earliest framboidal pyrite formed uniformly throughout the sediment prior to concretionary growth by the bacterial reduction of seawater sulfate in a pore water with free diffusive connection to the overlying seawater. Later euhedral pyrite nucleated on the framboids and is progressively more abundant toward the concretion margin. The isotopic composition of euhedral pyrite indicates formation by sulfate reduction in a pore system with restricted access to seawater sulfate, such that rates of sulfate reduction exceeded diffusive supply from seawater.

2. The formation of framboidal pyrite apparently utilized sources of iron within the concretionary horizon, probably by micro-scale diffusion to point sources of sulfate reduction. By contrast the formation of euhedral pyrite required transportation of iron from adjacent horizons. Similar patterns of iron and sulfur migration have been modelled by Berner (1969b) in sediments with a high reactive iron content and a heterogeneous organic matter distribution. Both conditions are satisfied by the Jet Rock concretions; the siting of these microbiologically-formed concretions is controlled by the presence of local concentrations of organic matter, and the molar ratio of reactive iron to reducible sulfur in the sediment exceeds 10 at deposition. The models predict that the pyritization of large, in situ sources of reactive iron allows sufficient time for other reduced products of bacterial decay to solubilize iron from adjacent sediments, as was observed to occur during formation of euhedral pyrite in the Jet Rock.

3. The observed changes in iron availability and pyrite crystallinity in passing from framboidal to euhedral pyrite are consistent with decreasing levels of saturation with respect to iron sulfides and a kinetic influence on pyrite texture. Initially, the combination of abundant in situ reactive iron and a rapid build-up of H_2S may cause supersaturation with respect to both mackinawite and pyrite. Despite the greater supersaturation with respect to pyrite, preferential precipitation of mackinawite may occur (Goldhaber and Kaplan, 1974). Subsequent transformation to greigite would then lead to framboidal pyrite. The resulting decrease in degree of supersaturation due to precipitation and declining iron availability may result in mackinawite becoming undersaturated, while pyrite is still supersaturated. Direct precipitation of pyrite would then give relatively coarse, well-crystallized euhedral material.

4. Isotopic and textural data can be combined to recognize four different types of pyrite, which can be arranged in a paragenetic sequence. The order of appearance and relative proportions of the different textural

and isotopic phases are controlled by those factors that affect the rate and magnitude of sulfate reduction (availability of sulfate, rate of sediment deposition, concentration of metabolizable organic matter) and the extent of iron sulfide supersaturation (pore water sulfide concentrations, availability of in situ reactive iron, availability of reactive iron in adjacent sediments).

ACKNOWLEDGMENTS

Textural observations were made by P. R. Simpson, Institute of Geological Sciences, London. His assistance and the helpful discussions with M. L. Coleman are gratefully acknowledged. The paper was first presented at the Third International Symposium on Water-Rock Interaction, Edmonton, 1980 and has since been modified considerably by constructive refereeing.

REFERENCES

Berner, R. A., 1964a, An idealized model of dissolved sulfate distribution in recent sediments: Geochim. et Cosmochim. Acta, v. 28, p. 1497-1503.

———— 1964b, Distribution and diagenesis of sulfur in some sediments from the Gulf of California: Marine Geology, v. 1, p. 117-140.

———— 1967, Thermodynamic stability of sedimentary iron sulfides: Am. Jour. Sci., v. 265, p. 773-785.

———— 1968, Calcium carbonate concretions formed by the decomposition of organic matter: Science, v. 159, p. 195-197.

———— 1969a, The synthesis of framboidal pyrite: Econ. Geology, v. 64, p. 383-384.

———— 1969b, Migration of iron and sulfur within anaerobic sediments during early diagenesis: Am. Jour. Sci., v. 267, p. 19-42.

———— 1970, Sedimentary pyrite formation: Am. Jour. Sci., v. 268, p. 1-23.

———— 1974, Kinetic models for the early diagenesis of nitrogen, sulfur, phosphorus and silicon in anoxic marine sediments, *in* Goldberg, E. D., ed., The Sea, v. 5: New York, John Wiley & Sons, p. 427-450.

———— 1978, Sulfate reduction and the rate of deposition of marine sediments: Earth Planetary Sci. Letters, v. 37, p. 492-498.

Berner, R. A., Scott, M. R., and Thomlinson, C., 1970, Carbonate alkalinity in the pore waters of anoxic marine sediments: Limnology Oceanography, v. 15, p. 544-549.

Coleman, M. L., and Raiswell, R., 1981, Carbon, oxygen, and sulfur isotope variations in carbonate concretions from the Upper Lias of NE England: Geochim. et Cosmochim. Acta, v. 45, p. 329-340.

Emery, K. O., 1960, The Sea off Southern California: New York, John Wiley & Sons, 366 p.

Farrand, M., 1970, Framboidal pyrites precipitated synthetically: Mineralium Deposita, v. 5, p. 237-247.

Goldhaber, M. B., and Kaplan, I. R., 1974, The sulfur cycle, *in* Goldberg, E. D., ed., The Sea, v. 5: New York, John Wiley & Sons, p. 569-655.

———— 1975, Controls and consequences of sulfate reduction rates in recent marine sediments: Soil Science, v. 119, p. 42-55.

Hallam, A., 1975, Jurassic Environments: Cambridge, Cambridge Univ. Press, 269 p.

Hallberg, R. O., 1972, Iron and zinc sulfides formed in a continuous culture of sulfate-reducing bacteria: Neues Jahrb. Mineralogie, v. 11, p. 481-500.

Harrison, A. G., and Thode, H. G., 1958, Mechanism of the bacterial reduction of sulfate from isotope fractionation studies: Faraday Soc. Trans., v. 54, p. 84-92.

Hartmann, U. M., and Nielsen, H., 1969, $\delta^{34}S$ werte in rezenten meeressedimenten und ihre deutung am beispiel einiger sedimentprofile aus der west lichen ostee: Geol. Rundschau, v. 58, p. 621-655.

Holser, W. T., and Kaplan, I. R., 1966, Isotope geochemistry of sedimentary sulfates: Chem. Geology, v. 1, p. 93-135.

Howarth, M. K., 1962, The Jet Rock Series and Alum Shale Series of the Yorkshire coast: Yorkshire Geol. Soc. Proc., v. 33, p. 381-422.

Jorgensen, B. B., 1979, A theoretical model of the stable sulfur isotope distribution in marine sediments: Geochim. et Cosmochim. Acta, v. 43, p. 363-374.

Kaplan, I. R., Emery, K. O., and Rittenberg, S. C., 1963, The distribution and isotopic abundance of sulfur in recent marine sediments off Southern California: Geochim. et Cosmochim. Acta, v. 27, p. 297-331.

Kaplan, I. R., and Rittenberg, S. C., 1964, Microbiological fractionation of sulfur isotopes: Jour. Gen. Microbiol., v. 34, p. 195-212.

Lippman, F., 1955, Ton, Geoden und Minerale des Barreme von Hoheneggelsen: Geol. Rundschau, v. 43, p. 475-503.

Love, L. G., 1957, Microorganisms and the presence of syngenetic pyrite: Geol. Soc. London Quart. Jour., v. 113, p. 429-440.

———— 1964, Early diagenetic pyrite in fine grained sediments and the genesis of sulfide ores, *in* Amstutz, G. C., ed., Sedimentology and Ore Genesis: Amsterdam, Elsevier, p. 11-17.

———— 1967, Early diagenetic iron sulfide in recent sediments of the Wash (England): Sedimentology, v. 9, p. 327-352.

Love, L. G., and Amstutz, G. C., 1966, Review of microscopic pyrite: Fortschr. Mineralogie, v. 43, p. 273-309.

Maxwell, J. A., 1968, Rock and Mineral Analysis: New York, Wiley-Intersci., 584 p.

Morris, K. A., 1979, A classification of Jurassic marine shale sequences: an example from the Toarcian (Lower Jurassic) of Great Britain: Paleogeography Paleoclimatology, Paleoecology, v. 26, p. 117-126.

———— 1980, Comparison of major sequences of organic-rich mud deposition in the British Jurassic: Geol. Soc. Jour., v. 137, p. 157-170.

Nakai, N., and Hensen, M. L., 1964, The kinetic isotope effect in the bacterial reduction and oxidation of sulfur: Geochim. et Cosmochim. Acta, v. 28, p. 1893-1912.

Presley, B. J., and Kaplan, I. R., 1968, Changes in dissolved sulfate, calcium and carbonate from interstitial water of near-shore sediments: Geochim. et Cosmochim. Acta, v. 32, p. 1037-1048.

Raiswell, R., 1971, The growth of Cambrian and Liassic concretions: Sedimentology, v. 17, p. 147-171.

———— 1976, The microbiological formation of carbonate concretions in the Upper Lias of NE England: Chem. Geology, v. 18, p. 227-244.

Raiswell, R., and Plant, J., 1980, The incorporation of trace elements into pyrite during diagenesis of black shales: Econ. Geology, v. 75, p. 684-699.

Raiswell, R., and White, N. H. M., 1978, Spatial aspects of concretionary growth in the Upper Lias of NE England: Sedimentary Geology, v. 20, p. 291-300.

Rees, C. E., 1973, A steady state model for sulfur isotope fractionation in bacterial reduction processes: Geochim. et Cosmochim. Acta, v. 37, p. 1141-1162.

Rickard, D. T., 1970, The origin of framboids: Lithos, v. 3, p. 269-293.

———— 1974, Kinetics and mechanism of the sulfidation of goethite: Am. Jour. Sci., v. 274, p. 941-952.

———— 1975, Kinetics and mechanism of pyrite formation at low temperatures: Am. Jour. Sci., v. 275, p. 635-652.

Riley, J. P., 1958, The rapid analysis of silicate rocks and minerals: Analytica Chim. Acta, v. 19, p. 413-428.

Robinson, B. W., and Kusakabe, M., 1975, Quantitative preparation of sulfur dioxide, for $^{34}S/^{32}S$ analysis, from sulfides by combustion with cuprous oxide: Anal. Chem., v. 47, p. 1179-1181.

Schwarz, H. P., and Burnie, S. W., 1973, Influence of sedimentary environments on sulfur isotope ratios in clastic rocks: a review: Mineralium Deposita, v. 8, p. 264-277.

Sweeney, R. E., and Kaplan, I. R., 1973, Pyrite framboid formation: laboratory synthesis and marine sediments: Econ. Geology, v. 68, p. 618-634.

Toth, D. J., and Lerman, A., 1977, Organic matter reactivity and sedimentation rates in the ocean: Am. Jour. Sci., v. 277, p. 465-485.

Trudinger, P. A., and Chambers, L. A., 1973, Reversibility of bacterial sulfate reduction and its relevance to isotope fractionation: Geochim. et Cosmochim. Acta, v. 37, p. 1775-1778.

Weeks, L. G., 1953, Environment and mode of origin and facies relationships of carbonate concretions in shales: Jour. Sed. Pet., v. 23, p. 162-173.

———— 1957, Origin of carbonate concretions in shales, Magdalena Valley, Columbia: Geol. Soc. America Bull., v. 68. p. 95-102.

Zangerl, R., Woodland, B. G., Richardson, Jr., E. S., and Zachary, Jr., D. L., 1969, Early diagenetic phenomena in the Fayetteville Black Shale (Mississippian) of Arkansas: Sedimentary Geology, v. 3, p. 87-119.